JOURNAL OF CATALYSIS 104, 99–108 (1987)

Stability of Model V–P–O Catalysts for Maleic Anhydride Synthesis

T. P. MOSER AND G. L. SCHRADER[1]

Department of Chemical Engineering and Ames Laboratory—U.S. Department of Energy, Iowa State University, Ames, Iowa 50011

Received June 6, 1986; revised September 30, 1986

The stability of β-$VOPO_4$ and $(VO)_2P_2O_7$ under conditions of n-butane and 1-butene oxidation was investigated using the complementary techniques of *in situ* laser Raman spectroscopy, X-ray diffraction, and X-ray photoelectron spectroscopy. Both β-$VOPO_4$ and $(VO)_2P_2O_7$ demonstrated bulk structural integrity during n-butane oxidation. The relatively greater reducing capacity of 1-butene, however, induced a transformation of β-$VOPO_4$ to $(VO)_2P_2O_7$. The presence of V(V) and V(IV) in used β-$VOPO_4$ and $(VO)_2P_2O_7$ was detected by X-ray photoelectron spectroscopy for both hydrocarbon oxidation conditions.

1. INTRODUCTION

Vanadium–phosphorus oxides have a special application as catalysts for the selective oxidation of C_4 hydrocarbons to maleic anhydride. An extensive body of literature has reported the preparation, characterization, and catalytic evaluation of various V–P–O phases. Some of the crystalline phases that have been identified include α-$VOPO_4$ (*1–3*), α_{II}-$VOPO_4$ (*4*), β-$VOPO_4$ (*2, 3, 5–7*), $(VO)_2P_2O_7$ (*2, 7, 8*), β-$(VO)_2P_2O_7$ (*9*), $VO(PO_3)_2$ (*2, 10*), and $VPO_5 \cdot 2H_2O$ (*11*). Recently, Bordes and Courtine (*12*) discussed three additional phases: δ-$VOPO_4$, γ-$VOPO_4$, and γ-$(VO)_2P_2O_7$. The structure and composition of more typical industrial catalysts revealed in the patent literature (such as the B-phase (*13*)) are poorly understood. It has been shown, however, that the B-phase and $(VO)_2P_2O_7$ have similar X-ray diffraction patterns, although the assigned structures differ.

The stability of V–P–O catalysts during C_4 hydrocarbon oxidation appears to depend strongly on the reducing environment. Investigators have principally determined phase stability by comparing X-ray diffraction patterns before and after C_4 hydrocarbon oxidation. Phases with the reduced V(IV) oxidation state, such as β-$(VO)_2P_2O_7$ (*9*) and the B-phase (*14*), were reported to be stable under n-butane oxidation conditions. In addition, Moser and Schrader (*7*) provided initial findings that β-$VOPO_4$ (a highly oxidized V(V) phase) and $(VO)_2P_2O_7$ were stable during n-butane oxidation. In contrast, Bordes and Courtine (*2*) used X-ray diffraction before and after catalyst use to demonstrate that α-$VOPO_4$ and β-$VOPO_4$ were reduced to $(VO)_2P_2O_7$ under 1-butene oxidation conditions. The bulk structural integrity of industrial B-phase (V(IV)) catalysts following 1-butene oxidation was suggested by Cavani *et al.* (*15*).

A crucial question regarding selective oxidation by V–P–O catalysts is the nature of the active phase(s) during actual reaction conditions. An initial report of the characterization of functioning β-$VOPO_4$ and $(VO)_2P_2O_7$ using *in situ* laser Raman spectroscopy has been provided by Moser and Schrader (*7*). The bulk structure of these compounds remained stable during n-butane oxidation. In this paper, further characterization of the stability of β-$VOPO_4$ and $(VO)_2P_2O_7$ for paraffin and olefin oxidation using *in situ* laser Raman spectroscopy, X-ray diffraction, and X-ray photoelectron

[1] To whom correspondence should be addressed.

0021-9517/87 $3.00

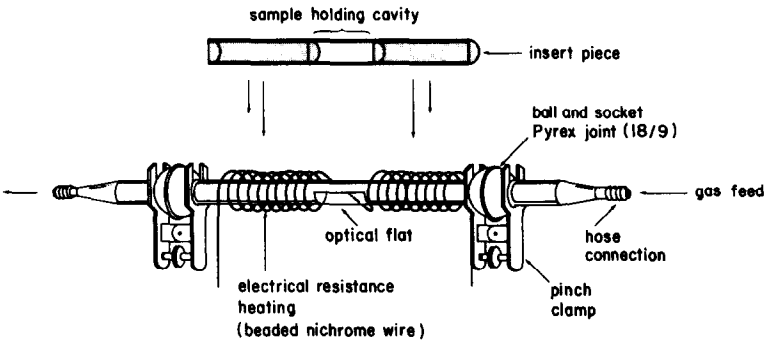

FIG. 1. Controlled atmosphere Raman cell.

spectroscopy is presented. These studies have provided new insight into the nature of the active oxygen involved in C_4 hydrocarbon oxidation.

2. EXPERIMENTAL PROCEDURE

2.A. Catalyst Preparation

Pure β-$VOPO_4$ and $(VO)_2P_2O_7$ were synthesized by solid-state reaction techniques described previously (*7*).

2.B. Catalyst Activity and Selectivity

The catalytic evaluation of β-$VOPO_4$ and $(VO)_2P_2O_7$ for n-butane conversion to maleic anhydride has been previously provided (*7*).

2.C. In Situ Laser Raman Spectroscopy of Functioning Catalysts

In situ laser Raman spectra of the functioning catalysts were obtained using a tubular controlled atmosphere cell (Fig. 1). The cell was constructed from a 8.5-cm section of 13-mm-o.d. standard-wall Pyrex tubing. An optically flat section (approximately 7 × 10 mm) of $\frac{1}{16}$-in.-thick borosilicate glass was fused to the center portion of the Pyrex tubing to serve as the cell window. The catalyst samples were held in an insert piece constructed from a 9-mm Pyrex rod and a 9-mm-o.d. section of standard-wall Pyrex tubing. Sections of the Pyrex rod and tubing were cut and fused to form a sample holding cavity (see Fig. 1). Fresh powdered catalyst was packed firmly into this cavity to form a flat surface. The cell could be heated to temperatures as high as 550°C using electrical resistance heating. The temperature was determined by a subminiature thermocouple probe (Omega Engineering) placed inside the cell near the sample. A vertical mount with dual axis stages was used for alignment of the cell within the sample compartment.

A Spex 1403 laser Raman spectrometer was used with the 514.3-nm line of a Spectra Physics Model 164 argon ion laser operated at 100 mW at the source. No thermal or photochemical decomposition of the catalyst sample occurred under these conditions. A Nicolet 1180E computer system made spectra accumulation possible. Typically, ten scans were accumulated at 5 cm^{-1} resolution. However, it was necessary to acquire as many as 75 to 100 scans with a typical scan speed of 3.125 cm^{-1}/s to obtain acceptable signal-to-noise ratios for experiments conducted at temperatures above 450°C.

The composition and flow rate of the gases fed to the *in situ* cell were controlled by Tylan mass flow controllers (Model FC260) which were calibrated for each of the specific gases. The feed gas was delivered at 50 cm^3/min.

2.D. Characterization Techniques for Fresh and Used Catalysts

2.D.1. X-ray diffraction. X-ray powder diffraction measurements were made with a

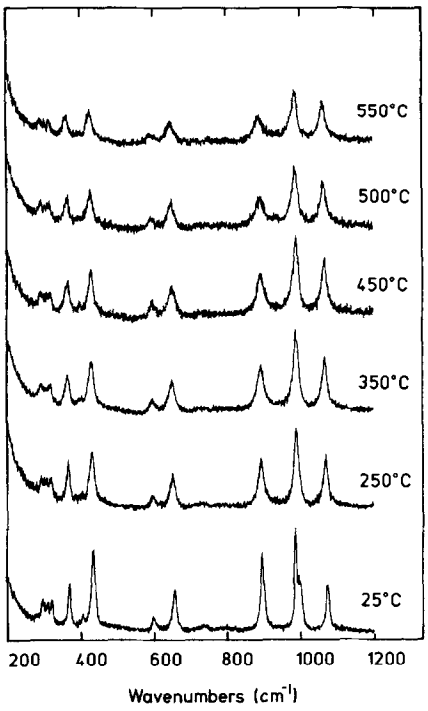

FIG. 2. *In situ* Raman spectra of β-$VOPO_4$: n-butane oxidation.

Siemans diffractometer with a preset spinning sample mount. Cu$K\alpha$ radiation was used.

2.D.2. X-ray photoelectron spectroscopy. X-ray photoelectron spectra were obtained for both fresh and used catalysts using an AEI 200B spectrometer with Al$K\alpha$ radiation. A Nicolet 1180 computer was used for data acquisition and for signal averaging. All spectra are referenced to the carbon 1*s* binding energy of 285 eV.

Catalysts exposed to both n-butane and 1-butene reaction conditions were prepared for XPS analysis in reactors constructed from 6-mm-o.d. standard-wall Pyrex tubing. Approximately 1 g of loosely packed fresh catalyst was charged to each reactor and plugged on either end with quartz wool. A reactant mixture of either 1.5% n-butane or 1-butene in dry air was passed over the catalyst bed (flow rate 50 cm^3/min). The catalyst bed was heated to 450°C in a split-tube furnace for 18 h. Used catalysts were cooled to room temperature in the feed mixture followed by sealing under vacuum in the Pyrex reactor tube. Fresh catalyst samples were similarly sealed under vacuum. Tubes containing both the fresh and used catalysts were opened in a helium dry box (oxygen free) attached directly to the spectrometer.

3. EXPERIMENTAL RESULTS

3.A. In Situ Characterization of Catalysts by Laser Raman Spectroscopy

3.A.1. Characterization of functioning β-$VOPO_4$. In situ Raman spectra of β-$VOPO_4$ were obtained under conditions for n-butane and 1-butene oxidation; the reducing effect of hydrogen was also examined.

Spectra for the β-$VOPO_4$ phase during exposure to 1.5% n-butane in air at temperatures from 25 to 550°C are given in Fig. 2. No new bands were observed even after 12 h of exposure. The shoulder band at 997 cm^{-1} was not observable at higher temperatures because of band broadening. The band width at one-half intensity of the 987 cm^{-1} peak was 11 cm^{-1} at room temperature; at temperatures 250°C and above, the band width increased to 17 cm^{-1}. A similar effect was noticed when fresh β-$VOPO_4$ was heated in a flow of air at 450°C. At room temperature, the β-$VOPO_4$ phase had a characteristic band at 1073 cm^{-1}. However, after heating the sample in the n-butane–air mixture at 450 to 550°C, the position of this band shifted to 1067 cm^{-1}. The same effect was also observed when β-$VOPO_4$ was heated in air at 450°C. The relative intensities of the bands at 896 and 987 cm^{-1} as compared to the intensity of the 1067-cm^{-1} band decreased during n-butane oxidation. All changes in the spectral features were reversible upon cooling to room temperature in the feed mixture.

Raman spectra of β-$VOPO_4$ were also accumulated using higher n-butane concentrations at 500°C. The Raman spectra remained relatively insensitive to changes in the gas feed composition.

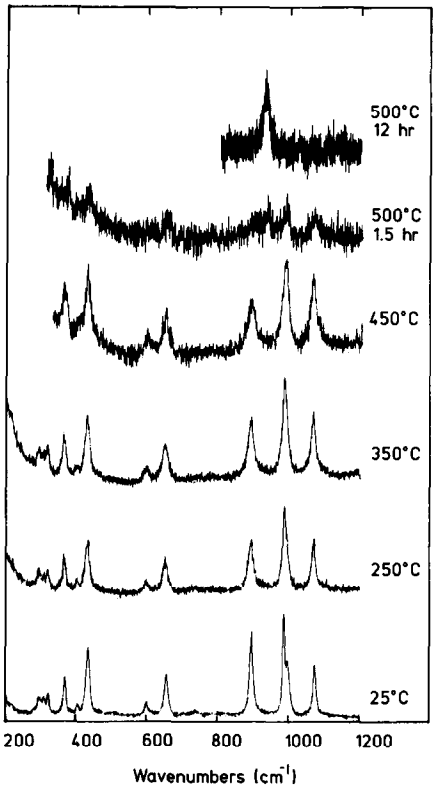

FIG. 3. *In situ* Raman spectra of β-$VOPO_4$: 1-butene oxidation.

Raman spectra of β-$VOPO_4$ during exposure to 1.5% 1-butene in air at temperatures from 25 to 550°C are given in Fig. 3. The position of the β-$VOPO_4$ bands underwent subtle changes for temperatures from 250 to 450°C. As for the n-butane experiments and for simple heating in air, the half-width of the 987-cm^{-1} band increased from 11 cm^{-1} to 18 cm^{-1}, with an apparent disappearance of the shoulder band at 997 cm^{-1}. The band at 1073 cm^{-1} also shifted to 1067 cm^{-1} upon heating. The relative intensities of the 896- and 987-cm^{-1} bands compared to that for the 1067-cm^{-1} band decreased between 250 to 450°C.

However, there were striking changes in the spectrum at 500°C for 1-butene oxidation after 1.5 h. The appearance of a new band at 932 cm^{-1} was observed with a considerable decrease in the intensity of the bands at 894, 987, and 1063 cm^{-1}. This new

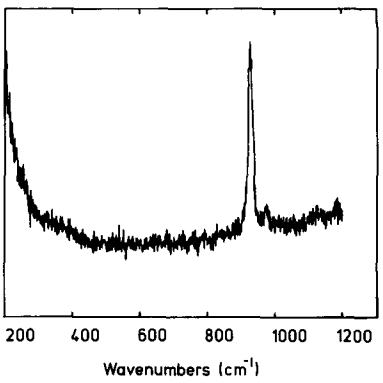

FIG. 4. Raman spectrum of used β-$VOPO_4$ after 1-butene oxidation.

band was characteristic of the reduced phase $(VO)_2P_2O_7$. After continued 1-butene oxidation for 12 h, only a single band at 932 cm^{-1} could be observed. This particular spectrum required 40 scans at a scan drive of 1.043 cm^{-1}/s. After 24 h of 1-butene oxidation the sample was cooled to room temperature under continued flow of the 1-butene–air mixture. As shown in Fig. 4, bands for the original β-$VOPO_4$ phase were not restored.

The Raman spectrum of β-$VOPO_4$ was also collected during exposure to hydrogen at 450°C. Figure 5 shows the 800 to 1200-cm^{-1} region of the Raman spectrum of β-$VOPO_4$ after 4 h of hydrogen reduction. The same subtle changes in the Raman spectrum were observed as for the n-butane

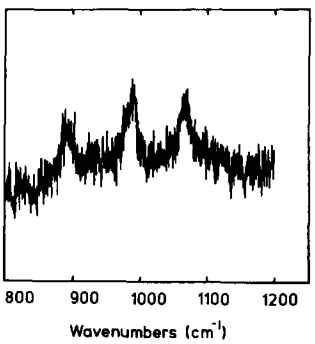

FIG. 5. *In situ* Raman spectrum of β-$VOPO_4$ during hydrogen reduction at 450°C.

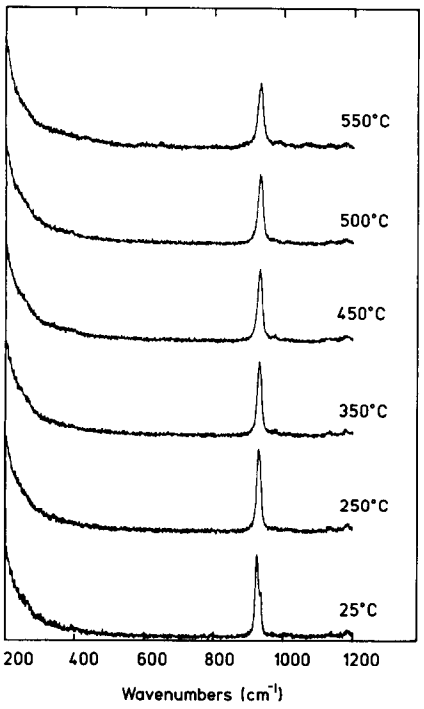

FIG. 6. *In situ* Raman spectra of $(VO)_2P_2O_7$: n-butane oxidation.

studies. After cooling to room temperature, all bands characteristic of fresh β-$VOPO_4$ were observable. However, the sample color changed from yellow-green to black. A decreased signal-to-noise ratio was also observed as compared to the spectrum of a fresh β-$VOPO_4$ sample.

3.A.2. Characterization of functioning $(VO)_2P_2O_7$. *In situ* Raman spectra of $(VO)_2P_2O_7$ were accumulated during both n-butane and 1-butene oxidation; the effect of exposure to oxygen at elevated temperatures was also examined.

The spectra of the functioning $(VO)_2P_2O_7$ phase (1.5% hydrocarbon in air) during both n-butane and 1-butene oxidation are given in Figs. 6 and 7, respectively. The Raman spectra were very similar for both cases. Two major bands were located at 921 and 932 cm^{-1}. After heating between 250 to 550°C, however, these bands evolved to a single band with a maximum at 930 cm^{-1}. At room temperature the band at 921 cm^{-1} had a half-width of 11 cm^{-1}. The band at 930 cm^{-1}, for spectra accumulated between 250 and 550°C, had a half-width of 16 cm^{-1}. These changes were reversible upon cooling to room temperature. No significant loss in the absolute intensities (photon counts/s) or the signal-to-noise ratio was observed during either n-butane of 1-butene oxidation. Weak bands characteristic of $(VO)_2P_2O_7$ persisted at elevated temperatures as high as 550°C.

The effect of heating $(VO)_2P_2O_7$ in a flow of oxygen was also studied; Raman spectra acquired at 450 to 550°C are given in Fig. 8. Distinct changes in the spectrum were apparent, particularly with the detection of a number of new bands not characteristic of $(VO)_2P_2O_7$. After 1.5 h of oxygen flow at 450°C, a broad feature between 250 to 550 cm^{-1} was observable. The band at 930 cm^{-1}, characteristic of the $(VO)_2P_2O_7$ phase for elevated temperatures, remained prominent during oxygen flow at 450°C. After 1.5

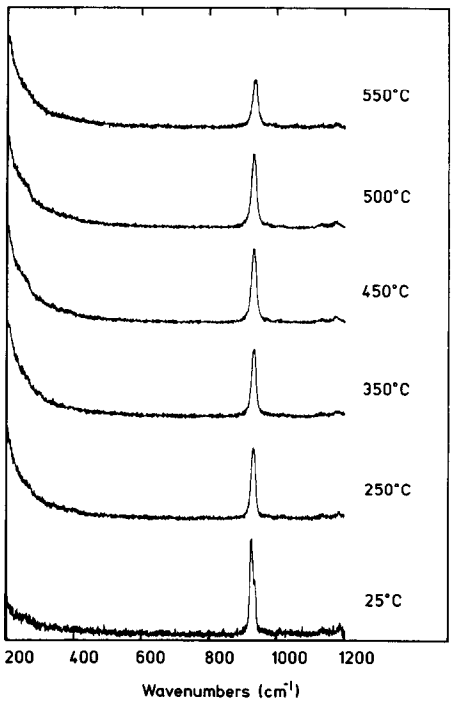

FIG. 7. *In situ* Raman spectra of $(VO)_2P_2O_7$: 1-butene oxidation.

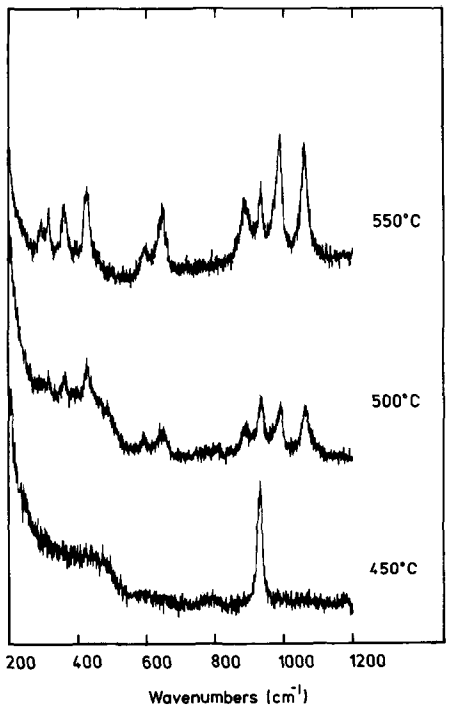

FIG. 8. Calcination of $(VO)_2P_2O_7$ in oxygen.

h of oxygen flow at 500°C, however, distinct bands appeared at 320, 369, and 435 cm^{-1} (Fig. 8). Other bands at 598, 651, 895, 987, and 1069 cm^{-1} also evolved with intensities comparable to the $(VO)_2P_2O_7$ peak at 930 cm^{-1}. These bands were characteristic of β-$VOPO_4$. Upon increasing the temperature to 550°C for 12 h these new bands became dominant, although there was clear evidence of the 930-cm^{-1} band. After cooling to room temperature, relatively larger amounts of β-$VOPO_4$ were apparent.

3.B. Characterization of Used Catalysts

3.B.1. X-ray diffraction. The X-ray diffraction patterns of β-$VOPO_4$ after n-butane and 1-butene oxidation were compared to that of fresh material. The d-spacings for fresh β-$VOPO_4$ and for the catalyst after 1-butene oxidation are given in Table 1. No changes were observed after n-butane oxidation performed at 425 to 525°C. However, the X-ray data did show a phase transformation from β-$VOPO_4$ to $(VO)_2P_2O_7$ after 1-butene oxidation between 500 and 550°C. The primary diffraction lines of β-$VOPO_4$ were not preserved (*d*-spacings 3.078, 3.196, and 3.416 Å); rather, the presence of the $(VO)_2P_2O_7$ phase was indicated by three intense diffraction lines (among other weaker lines) at 2.989, 3.143, and 3.886 Å (*2, 7*). After cooling to room temperature, the diffraction pattern of used β-$VOPO_4$ clearly showed a considerable amount of crystalline $(VO)_2P_2O_7$.

X-ray diffraction confirmed that $(VO)_2P_2O_7$ was remarkably stable during the high temperature (425 to 525°C) oxidation of both n-butane and 1-butene. A distinct phase transformation to β-$VOPO_4$ was observed, however, when $(VO)_2P_2O_7$ was heated in a flow of oxygen. Samples were obtained from the *in situ* Raman spectroscopy studies described previously when $(VO)_2P_2O_7$ was heated in oxygen at 500 and 550°C. The *d*-spacings are given in Table 1 together with relative line intensities.

3.B.2. X-ray photoelectron spectroscopy (XPS). X-ray photoelectron spectra of both fresh and used catalysts are shown in Figs. 9 and 10; Table 2 provides the observed

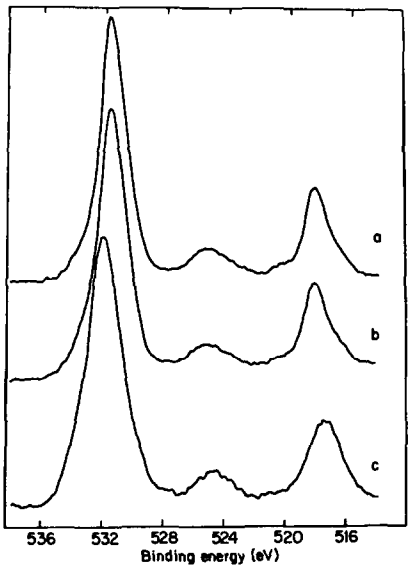

FIG. 9. X-ray photoelectron spectra of fresh and used β-$VOPO_4$ (a) fresh; (b) after n-butane oxidation; (c) after 1-butene oxidation.

TABLE 1

X-ray Diffraction Patterns of Fresh and Used Catalysts

d-spacing (Å)	Relative intensity	*d*-spacing (Å)	Relative intensity	*d*-spacing (Å)	Relative intensity	*d*-spacing (Å)	Relative intensity	*d*-spacing (Å)	Relative intensity	*d*-spacing (Å)	Relative intensity
Fresh β-$VOPO_4$		Fresh $(VO)_2P_2O_7$		β-$VOPO_4$, after 1-butene oxidation 500°C		β-$VOPO_4$ after 1-butene oxidation 550°C		$(VO)_2P_2O_7$ after oxygen flow 500°C		$(VO)_2P_2O$ after oxygen flow 550°C	
5.233	31.6	6.323	14.4	6.299	9.2	6.298	12.7	6.301	11.2	6.295	11.1
4.629	31.5	5.707	14.7	5.675	9.1	5.695	12.4	5.693	15.6	5.680	13.5
3.985	11.0	4.826	13.9	4.805	15.2	4.812	12.4	5.233	8.1	5.214	30.8
3.903	23.6	4.090	6.2	3.976	15.5	3.975	7.5	4.919	6.7	4.799	12.6
3.501	23.4	3.889	100.0	3.885	100.0	3.886	100.0	4.815	13.6	4.617	26.5
3.416	100.0	3.147	88.8	3.317	17.3	3.299	8.1	4.624	6.6	4.080	4.8
3.196	24.9	2.991	49.0	3.143	77.6	3.143	79.6	4.081	7.2	3.974	13.6
3.078	50.9	2.921	7.5	2.989	34.0	2.989	36.9	3.984	9.1	3.879	100.0
2.983	22.2	2.662	20.8	2.660	15.8	3.660	15.2	3.883	100.0	3.495	20.8
2.834	13.7	2.444	20.6	2.473	4.9	2.442	17.3	3.511	8.4	3.408	85.4
2.648	12.6	2.363	9.4	2.442	19.5	2.368	5.6	3.418	15.5	3.285	4.1
2.607	8.0	2.256	6.6	2.369	5.8	2.262	5.4	3.143	87.8	3.188	19.7
2.415	6.1	2.095	29.7	2.260	8.1	1.940	13.7	3.077	14.4	3.140	70.1
2.281	7.5	1.994	8.6	2.093	22.5	1.841	15.9	2.989	44.3	3.070	47.7
2.213	10.5	1.937	10.5	1.939	11.6	1.649	6.5	2.914	4.2	2.984	55.3
2.178	9.5	1.842	16.8	1.842	14.9	1.577	17.8	2.660	15.0	2.914	5.7
2.092	7.6	1.796	6.1	1.650	3.8	1.473	5.8	2.442	23.0	2.830	11.2
2.000	7.7	1.648	6.3	1.636	5.1	1.461	9.5	2.366	6.2	2.655	21.8
1.986	5.3	1.577	19.1	1.599	4.3			2.254	7.9	2.606	4.5
1.965	14.9	1.475	8.4	1.578	18.8			2.209	4.9	2.460	5.6
1.751	7.6	1.460	10.7	1.474	4.9			2.093	23.5	2.440	13.9
1.726	7.5			1.461	5.8			1.995	4.6	2.404	5.7
1.703	6.9							1.965	6.6	2.364	5.1
1.641	8.6							1.937	10.2	2.278	5.8
1.607	12.7							1.709	6.1	2.255	4.6
1.538	30.9							1.646	5.6	2.209	11.0
								1.637	6.1	2.176	10.6
								1.599	6.0	2.092	31.0
								1.578	12.8	1.994	13.7
								1.475	8.6	1.962	16.3
								1.460	6.9	1.946	5.3
										1.937	8.5
										1.886	4.2
										1.840	11.2
										1.795	5.0
										1.750	8.7
										1.725	4.9
										1.702	11.0
										1.646	7.8
										1.606	4.3
										1.601	5.6
										1.576	10.9
										1.537	25.5
										1.474	6.3
										1.459	9.8

binding energies. The β-$VOPO_4$ phase was characterized by two bands at 518.2 and 525.6 eV which were assigned to the $2p_{3/2}$ and $2p_{1/2}$ binding energies of V(V), respectively. The oxygen 1*s* binding energy for β-$VOPO_4$ was 531.4 eV. The XPS spectra for $(VO)_2P_2O_7$ had two bands at 517.1 and 524.4 eV, which were assigned to the $2p_{3/2}$ and $2p_{1/2}$ binding energies of V(IV), respectively. An oxygen 1*s* binding energy was observed at 531.5 eV. Similar results for these phases were reported by Shimoda *et al.* (*16*).

Following n-butane oxidation, the XPS spectra for β-$VOPO_4$ showed a −0.3-eV shift for the bands associated with the vanadium $2p_{3/2}$ and $2p_{1/2}$ binding energies. After 1-butene oxidation, the β-$VOPO_4$ phase spectra exhibited shifts for both vanadium $2p_{3/2}$ (−0.8-eV) and vanadium $2p_{1/2}$ (−0.8-

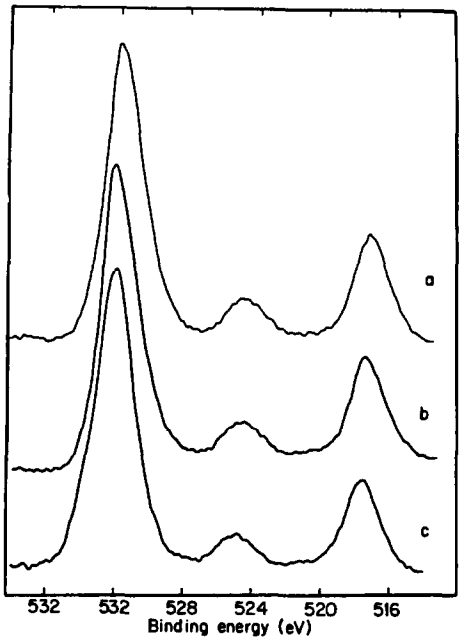

FIG. 10. X-ray photoelectron spectra of fresh and used $(VO)_2P_2O_7$ (a) fresh; (b) after n-butane oxidation; (c) after 1-butene oxidation.

eV) peaks and the oxygen 1*s* (+0.6-eV) peak. The band half-widths of the vanadium $2p_{3/2}$ and oxygen 1*s* binding energies also broadened by 0.6 eV. The XPS spectra of $(VO)_2P_2O_7$ showed small changes in peak locations following both n-butane and 1-butene oxidation. A shift occurred for the vanadium $2p_{3/2}$ (+0.3-eV) and $2p_{1/2}$ (+0.2-eV) peaks with a simultaneous shift for the oxygen 1*s* (+0.4-eV) peak following n-butane oxidation. The vanadium $2p_{3/2}$ band broadened by about 0.3 eV. The magnitude of the binding energy shifts were comparable following 1-butene oxidation for the vanadium $2p_{3/2}$ (+0.4-eV) and $2p_{1/2}$ (0.4-eV) peaks for the oxygen 1*s* (0.4-eV) peak.

TABLE 2

Photoelectron Spectra Binding Energies for Fresh and Used Catalysts (eV)

Sample	V $2p_{3/2}$	V $2p_{1/2}$	O 1*s*
β-$VOPO_4$	518.2 (1.6)	525.6 (2.1)	531.4 (2.0)
After n-butane oxidation	517.9 (1.8)	525.3 (2.2)	531.3 (2.2)
After 1-butene oxidation	517.4 (2.2)	524.8 (2.0)	532.0 (2.6)
$(VO)_2P_2O_7$	517.1 (2.0)	524.4 (2.4)	531.5 (2.4)
After n-butane oxidation	517.4 (2.3)	524.6 (2.1)	531.9 (2.7)
After 1-butene oxidation	517.5 (2.1)	524.8 (2.2)	531.9 (2.4)

Note. Binding energies are referenced to carbon 1*s* of 285 eV. Half-widths (eV) are given in parentheses.

4. DISCUSSION OF RESULTS

The stability of the β-$VOPO_4$ and $(VO)_2P_2O_7$ crystalline phases under conditions associated with n-butane and 1-butene oxidation was investigated using the complementary techniques of laser Raman spectroscopy, X-ray diffraction, and X-ray photoelectron spectroscopy. The Raman technique was particularly important because of its utility as an *in situ* technique. X-ray diffraction data from postreactor samples confirmed the Raman results with respect to bulk structural stability and transformations. Questions regarding the catalyst oxidation states were addressed using XPS.

The β-$VOPO_4$ and $(VO)_2P_2O_7$ bulk structures were remarkably stable during n-butane oxidation between 25 and 550°C as indicated by *in situ* laser Raman spectroscopy and postcatalytic X-ray diffraction measurements. Modifications in the Raman spectra for β-$VOPO_4$ could be observed, however. The bands associated with β-$VOPO_4$ decreased in intensity by about a factor of 10 over the temperature range from 25 to 550°C. This decreased signal implied that some reduction occurs, but not sufficiently throughout the entire catalyst bulk structure such that a distinct reduced V–P–O phase was formed. The decrease in the relative intensities of the bands at 896 and 987 cm^{-1} as compared to the intensity of band at 1067 cm^{-1} implied that localized reduction occurred involving specific sites in the β-$VOPO_4$ lattice. The bands at 896 and 987 cm^{-1} have been associated with P–O stretches of the PO_4 units of β-$VOPO_4$. Detailed band assignments were discussed previously by Moser and Schrader (*7*). The $(VO)_2P_2O_7$ phase did not show a significant loss in Raman band intensities. Bulk reduction of $(VO)_2P_2O_7$ re-

duction to a V(III) phase apparently does not occur.

X-ray photoelectron spectra of both β-$VOPO_4$ and $(VO)_2P_2O_7$ following n-butane oxidation at 450°C did show modifications in the oxidation state of the catalysts. The β-$VOPO_4$ phase was slightly reduced as indicated by a −0.3-eV shift for the binding energy of the vanadium $2p_{3/2}$ electrons. This band shift was accompanied by a slight broadening (0.2 eV). Conversely, $(VO)_2P_2O_7$ was slightly oxidized as indicated by a shift in the binding energy of the vanadium $2p_{3/2}$ band from 517.1 to 517.4 eV, together with a broadening of the band (0.3 eV). These binding energy shifts probably correspond to the presence of both V(V) and V(IV). The magnitude of these shifts, however, suggest that the corresponding reduction or oxidation was rather small. Postcatalytic characterization by both Raman spectroscopy and X-ray diffraction indicated no bulk structural changes.

Transformation from β-$VOPO_4$ to $(VO)_2P_2O_7$ was clearly detected during 1-butene oxidation between 450 to 550°C as indicated by *in situ* laser Raman spectroscopy and postcatalytic characterization using X-ray diffraction. X-ray photoelectron spectroscopy showed further that the β-$VOPO_4$ phase was reduced during 1-butene oxidation in air at 450°C as indicated by shift in the vanadium $2p_{3/2}$ binding energy from 518.2 to 517.4 eV. This shift was accompanied by a rather significant broadening of both the vanadium $2p_{3/2}$ and vanadium $2p_{1/2}$ bands (0.6 eV), indicating that both V(V) and V(IV) were present. In comparison, $(VO)_2P_2O_7$ underwent a small, yet significant, oxidation during 1-butene oxidation. The binding energy for the vanadium $2p_{3/2}$ electrons shifted from 517.1 to 517.5 eV.

When β-$VOPO_4$ was charged to the *in situ* Raman cell bands characteristic of both β-$VOPO_4$ and $(VO)_2P_2O_7$ were present during 1-butene oxidation in air. After continued 1-butene oxidation at 500°C for 12 h, the β-$VOPO_4$-to-$(VO)_2P_2O_7$ transition was almost complete as indicated by a single band at 930 cm^{-1}, characteristic of $(VO)_2P_2O_7$ at elevated temperatures. In addition, the relative intensities of the P–O stretches at 896 and 987 cm^{-1} decreased as compared to the intensity of the band at 1067 cm^{-1} between 250 and 500°C. As during n-butane oxidation, it appears that oxygen vacancies were produced at P–O positions associated with the PO_4 units of β-$VOPO_4$. Because of the severity of the 1-butene reducing capacity, enough of these vacancies were created to allow the bulk restructuring to the reduced $(VO)_2P_2O_7$ phase at 500°C. In contrast, the reduction of β-$VOPO_4$ in hydrogen at 450°C was not accompanied by a phase transformation. *In situ* Raman spectra collected at 450°C in hydrogen showed bands characteristic of β-$VOPO_4$. The absolute intensities of these bands, however, were rather weak as compared to similar experiments with n-butane in air. The modifications in the Raman spectrum suggests that the catalyst was reduced, possibly to an amorphous structure present together with β-$VOPO_4$. X-ray diffraction has confirmed the reduction of β-$VOPO_4$ in hydrogen can produce an amorphous material (*7*).

The thermal heating of either β-$VOPO_4$ or $(VO)_2P_2O_7$ at 250°C and above caused broadening of the Raman bands with or without n-butane or 1-butene being present. *In situ* laser Raman spectroscopy identified this change for β-$VOPO_4$ by the merging of the P–O band at 987 cm^{-1} with the V=O band at 997 cm^{-1}. The center of the composite band was located at 987 cm^{-1} (250 to 550°C). Another subtle change was associated with the P–O stretch at 1073 cm^{-1} (25°C) which shifted to 1067 cm^{-1} (250 to 550°C). This shift was likewise attributed to thermal heating effects. Finally, the $(VO)_2P_2O_7$ phase was characterized by two intense P–O–P asymmetric stretches of the pyrophosphate ion at 921 and 932 cm^{-1}. These two bands merged at elevated temperatures to become a single band at 930

cm^{-1}. The changes in band structure associated with thermal heating were completely reversible upon cooling the phases to room temperature.

5. CONCLUSIONS

The present investigation has examined the stability of two model V–P–O phases, β-$VOPO_4$ and $(VO)_2P_2O_7$, using *in situ* laser Raman spectroscopy, X-ray diffraction, and X-ray photoelectron spectroscopy. The *in situ* Raman technique revealed key catalyst transformations that occurred during C_4 hydrocarbon oxidation which were otherwise undetectable by postcatalytic characterization. In particular, β-$VOPO_4$ and $(VO)_2P_2O_7$ demonstrated bulk structural integrity during n-butane oxidation. Modifications in the Raman spectra of functioning β-$VOPO_4$ indicated, however, that oxygen holes were created in the lattice of β-$VOPO_4$, causing a slight reduction without bulk restructuring. Furthermore, Raman band assignments indicated these oxygen sites were associated with PO_4 units in the lattice of β-$VOPO_4$. The severity of the reducing environment had a marked effect on the stability of the model compounds. A 2β-$VOPO_4 \rightarrow (VO)_2P_2O_7$ phase transformation was observed during 1-butene oxidation at 500°C. As for n-butane oxidation, oxygen vacancies were created at P–O positions in the lattice of β-$VOPO_4$; the reducing capacity of 1-butene, however, led to the specific phase transformation.

ACKNOWLEDGMENTS

This work was conducted through the Ames Laboratory which is operated for the U.S. Department of Energy by Iowa State University under Contract W-7405-ENG-82. The X-ray photoelectron spectroscopy work by James W. Anderegg is gratefully acknowledged.

REFERENCES

1. Jordan, B., and Calvo, C., *Canad. J. Chem.* **51,** 2621 (1973).
2. Bordes, E., and Courtine, P., *J. Catal.* **57,** 236 (1979).
3. Bordes, E., Courtine, P., and Pannetier, G., *Ann. Chim.* **8**(2), 105 (1973).
4. Tachez, M., Theobald, F., and Bordes, E., *J. Solid State Chem.* **40,** 280 (1981).
5. Brown, J., and Hummel, F., *Trans. Brit. Ceram. Soc.* **64,** 419 (1965).
6. Gopal, R., and Calvo, C., *J. Solid State Chem.* **5,** 432 (1972).
7. Moser, T., and Schrader, G., *J. Catal.* **92,** 216 (1985).
8. Gorbunova, Yu. E., and Linde, S. A., *Sov. Phys. Dokl.* **24,** (3) (1979).
9. Pepera, M., Callahan, J., Desmond, M., Milberger, E., Blum, P., and Bremer, N., *J. Amer. Chem. Soc.* **107,** 4884 (1985).
10. Tofield, B., Crane, G., Pasteur, G., and Sherwood, R., *J. C. S. Dalton,* 1806 (1975).
11. Ladwig, G., *Z. Anorg. Allg. Chem.* **338,** 266 (1965).
12. Bordes, E., and Courtine, P., *J. Chem. Soc., Chem. Commun.,* 294 (1985).
13. Schneider, R., U.S. Patent 3,864,286.
14. Centi, G., Fornasari, G., and Trifiro, F., *J. Catal.* **89,** 44 (1984).
15. Cavani, F., Centi, G., Manenti, I., and Trifiro, F., *Ind. Eng. Chem. Prod. Res. Dev.* **24,** 221 (1985).
16. Shimoda, T., Okuhara, T., and Misono, M., *Bull. Chem. Soc. Japan.* **58,** 2163 (1985).